FAST TRACK PAPER

Non-volcanic tremor beneath the Central Range in Taiwan triggered by the 2001 M_w 7.8 Kunlun earthquake

Zhigang Peng and Kevin Chao

School of Earth and Atmospheric Sciences, Georgia Institute of Technology, Atlanta, GA 30332, USA. E-mail: zpeng@gatech.edu

SUMMARY

Non-volcanic tremor (NVT) is an extended-duration and non-impulsive seismic signal observed away from volcanic regions. Although NVT has been found along the circum-Pacific subduction zones and the transform plate boundary in California, it is not clear whether NVT occurs in other tectonic environments. NVT is often associated with slow-slip events, and can be triggered instantaneously during the surface waves of teleseismic events. However, the underlying mechanisms of tremor generation remain mysterious. Here we show clear evidence of NVT beneath the Central Range (CR) in Taiwan triggered by the 2001 M_w 7.8 Kunlun earthquake in northern Tibet. Tremor occurs when the Love wave displacement is to the southwest (the lateral motion direction for the CR), suggesting a simple frictional response to the driving force. We hypothesize that tremor occurred on the weak basal detachment fault beneath the CR. Our observations indicate that tremor may exist at a wide range of active tectonic environments.

Key words: Earthquake interaction, forecasting, and prediction; Dynamics and mechanics of faulting; Rheology and friction of fault zones.

1 INTRODUCTION

Non-volcanic tremor (NVT) represents seismic signal observed away from volcanic regions with long durations, no clear body wave arrivals, and spectra depleted in high-frequency energy compared with regular earthquakes of similar amplitude. NVT was originally identified in the subduction zone southwest of Japan (Obara 2002), and subsequently found at many places along the circum-Pacific subduction zones (Rogers & Dragert 2003; Kao *et al.* 2005; Schwartz & Rokosky 2007), and along the San Andreas fault (SAF) system in California (Nadeau & Dolenc 2005). Recent studies also show that NVT can be triggered instantaneously during the surface waves of teleseismic events (Miyazawa & Mori 2005, 2006; Rubinstein *et al.* 2007; Gomberg *et al.* 2008; Miyazawa & Brodsky 2008; Peng *et al.* 2008).

So far NVT has been observed only in subduction zone and transform-fault environments. Some studies have proposed that NVT is generated by fluid migration due to dehydration from the subducted slabs (Obara 2002; Kao *et al.* 2005). Other recent studies suggested that much of tremor activity is superposition of many simple shear failure events on the plate interface (Shelly *et al.* 2007). Additional observations of tremor in diverse tectonic environments would help to better quantify the underlying mechanisms and necessary conditions for tremor generation.

Inspired by the recent observations of NVT in Vancouver Island (Rubinstein *et al.* 2007) and California (Gomberg *et al.* 2008; Peng

et al. 2008) triggered by the surface waves of the 2002 M_w 7.8 Denali earthquake, we examined seismic records in Taiwan (Fig. 1) generated by the 2001 M_w 7.8 Kunlun earthquake in northern Tibet. This earthquake is associated with a predominately unilateral rupture on the western segment of the Kunlun fault with a total length of more than 400 km (Lin *et al.* 2002). All these conditions help to generate large-amplitude surface waves in the rupture propagation direction.

We focus on the Island of Taiwan (Fig. 1) because of the following reasons. First, it is seismically active and has high-density seismic and geodetic networks, which provide ideal conditions for NVT and slow-slip events to be generated and observed. However, it is worth noting that ambient tremor and slow-slip events have not been observed before around Taiwan. In addition, the tectonic configuration around Taiwan is rather unique. The collision of the Chinese continental margin and the Luzon Arc results in the creation of the Central Range (CR) in Taiwan. Part of the deformation is consumed by left-lateral and thrust faulting along the Longitudinal Valley fault (LVF), which is a 160-km-long NNE-striking suture marking the boundary between the two plates in eastern Taiwan. The rest is accommodated by the fold-thrust belt that forms the Western Foothills (WF) of the CR (Fig. 1b). Observing NVT in an arc-continental type collision environment such as Taiwan would not only help to better understand necessary conditions relevant to tremor occurrence, but also improve our understanding of fault mechanics at the bottom of the seismogenic layer and of earthquake physics.
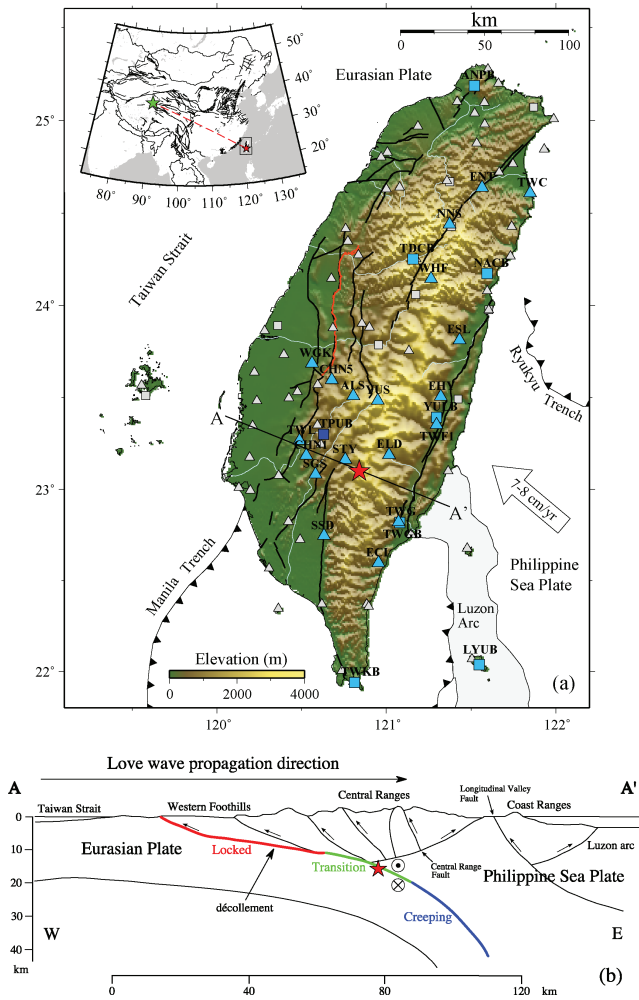
GJI Volcanology, geothermics, fluids and rocks

Figure 1. (a) Map of Taiwan. Seismic stations in the Broadband Array in Taiwan for Seismology (BATS) and short-period stations operated by the Central Weather Bureau (CWB) are denoted with squares and triangles, respectively. Stations marked with colours and station names are used for tremor locations. The broad-band station TPUB is shown as a blue square. The dark lines denote surface traces of active faults. The red line marks the surface trace of the 1999 M_w 7.6 Chi-Chi earthquake. The tremor location is denoted by the red star. The arrow marks the plate motion rate of 7–8 cm yr^{-1} from GPS data (Yu *et al.* 1997). The inset shows the epicentre of the 2001 M_w 7.8 Kunlun earthquake (green star), the tremor location (red star), and the great circle ray path. (b) A schematic cross-section of geological features in southern Taiwan along AA' in (a). The tremor location is marked by the red star. The red and blue colours mark the locked and creeping portion of the basal detachment fault, respectively. The green colour denotes the inferred transition zone where triggered tremor occurs. Modified from (Johnson *et al.* 2005).

2 OBSERVATIONS OF TRIGGERED TREMOR

In this study, we utilize the seismic data recorded by the Broadband Array in Taiwan for Seismology (BATS), and by short-period stations operated by the Central Weather Bureau (CWB). We identify NVT as bursts of non-impulsive seismic signals in the frequency range of 2–8 Hz that are coherent among many stations and are modulated by the surface waves. Fig. 2 shows a comparison of the transverse-component broad-band and 2–8 Hz bandpass-filtered velocity seismograms recorded at the BATS station TPUB. At low
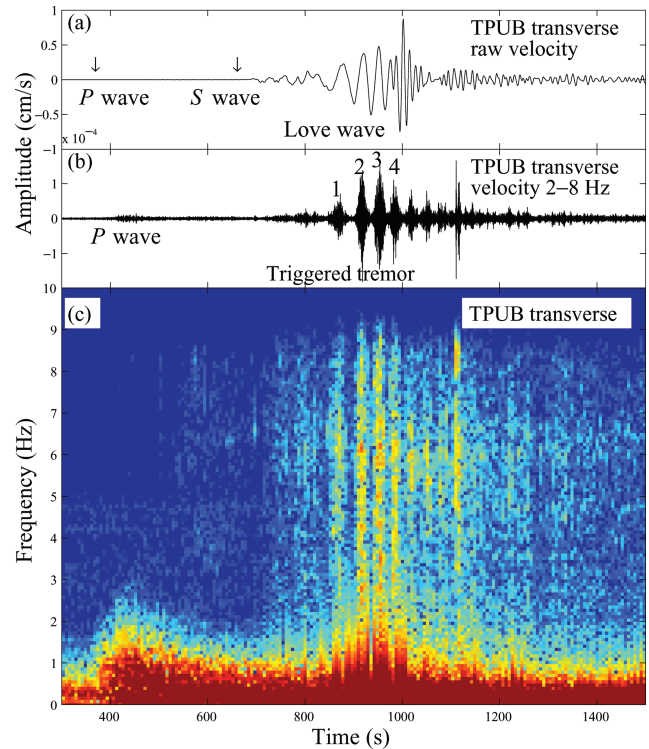

Figure 2. Examples of triggered tremor during the surface waves of the 2001 November 14 M_w 7.8 Kunlun earthquake. (a) Broad-band transverse-component seismogram recorded at station TPUB. The time is relative to the origin time of the Kunlun earthquake. The two arrows mark the approximate arrival time of the P and S waves. (b) 2–8 Hz bandpass-filtered transverse-component seismogram showing the high-frequency P waves and the triggered tremor during the passage of the Love waves. The location for the four tremor bursts with large amplitude is shown as red star in Fig. 1. (c) The spectrogram of the transverse-component seismogram at station TPUB. The triggered tremor signals are shown as narrow vertical bands rich in high-frequency energy as compared with the teleseismic P and surface waves.

frequencies, the Love waves are clearly visible. At high frequencies, we can identify the P waves, and bursts of energies between 800 and 1200 s during the large-amplitude Love waves. Because seismic waves are recorded on scale by both broad-band and short-period instruments, these high-frequency bursts are not caused by instrument clipping. In addition, each high-frequency burst is coherent among many stations that are several tens of kilometres away, and has clear shifts in time with distance (moveout), indicating a common origin for these events (Fig. S1, see Supporting Information online). The high-frequency burst has duration of 20–30 s, and appears to be symmetric in time with no identifiable P and S waves. Based on the similarities in both the characteristics and correlation with the surface waves as compared to triggered NVT observed in Cascadia (Rubinstein *et al.* 2007) and California (Gomberg *et al.* 2008), we attribute these bursts of high-frequency energies as NVT triggered by the surface waves of the Kunlun earthquake.

3 TREMOR LOCATIONS

We locate the first four bursts of tremor with the largest amplitude by minimizing the root-mean-square (rms) between the observed differential traveltimes measured by waveform cross correlations of tremor envelopes (Fig. S1, see Supporting Information online)
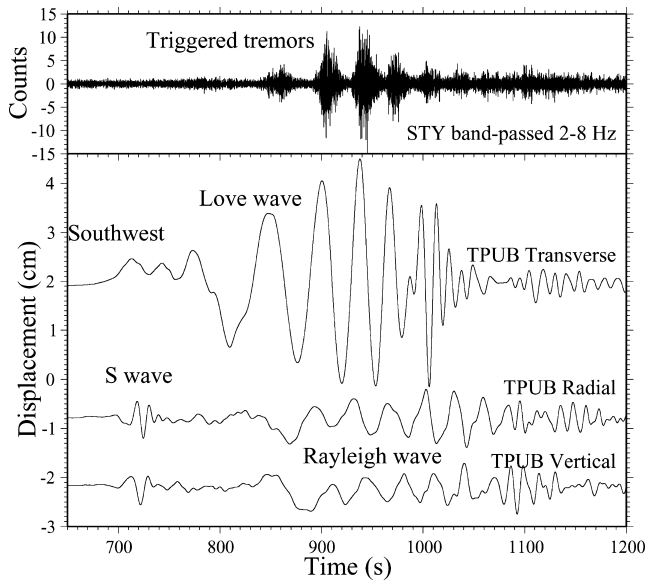
Figure 3. A comparison of the triggered tremor recorded at station STY and the three-component displacement seismograms at the BATS station TPUB after shifting them back to tremor source region.

and those computed from a 1-D velocity model in the region (Chen *et al.* 2001). The tremor location is tightly constrained to be at $120.84°E \pm 0.04°$ and $23.10°N \pm 0.04°$ underneath the CR. The depth is loosely constrained at 19 ± 6 km. We also locate the four bursts of tremor separately, and their locations are within 10 km of the best-fitting location, indicating that they may originate from the same place. Additional bursts are recorded by stations WHF, NNS and NACB in northeastern Taiwan and may correspond to different tremor sources; because the observed bursts do not follow the moveout from the southern source (Fig. S2, see Supporting Information online). We did not attempt to locate these tremor sources due to the relatively small number of observations.

4 CORRELATIONS BETWEEN NVT AND SURFACE WAVES

Next, we shift the tremor bursts and the surface waves back to the tremor source region to quantify their casual relationship (Fig. 3). We take the tremor bursts recorded by the nearest station STY, and apply a time shift of 6.8 s as computed from the best-fitting location and the 1-D velocity model. The surface waves recorded by the nearest broad-band stations TPUB are shifted by 7.3 s using a phase velocity of 4.1 km s^{-1} as measured from the 10 broad-band stations in the BATS array (Fig. S4, see Supporting Information online). Although both the Love and Rayleigh waves are in phase with the tremor bursts, the amplitudes of the Love waves are about 4 times larger than for the Rayleigh waves, suggesting that NVT is most likely triggered by stressing from the Love waves.

Assuming plane wave propagation, the peak dynamic stress σ_d associated with Love waves is proportional to $G\dot{u}/v_s$ (Jaeger & Cook 1979), where G is the shear modulus, $\dot{u}$ is the peak particle velocity, and v_s is the phase velocity (4.1 km s^{-1}). Using the peak particle velocity of $\sim$0.84 cm s^{-1} at station TPUB, and a nominal G value of 30 GPa, we estimate the amplitude of the stress levels associated with the Love waves to be $\sim$60 KPa, similar to those found in previous studies of triggered tremor (Rubinstein *et al.*

2007; Peng *et al.* 2008). We note that this value corresponds to stress levels on the surface, which could be different at depth. However, an increase of shear modulus with depth is often offset by a decrease of the Love wave peak velocity (Hill & Prejean 2007). Hence, the stress level is probably on the same order at the source region where NVT is generated.

5 INTERPRETATION

Elastic dislocation modelling of GPS data suggests that a basal detachment or décollement fault beneath the CR may be responsible for transferring the 3–4.5 cm yr^{-1} horizontal shortening to the WF (Dominguez *et al.* 2003; Johnson *et al.* 2005). Their results suggest that the detachment fault is locked in the front few tens of kilometres of the wedge, and is creeping in the deeper portion beneath the CR. Such basal detachment is considered to be a universal component of many fold-thrust belts, and can be well explained by a critical-taper wedge model (e.g. Davis *et al.* 1983). The décollement model contains a dip of 6° to the east for the basal detachment beneath the CR. The depth of detachment is found to be at $\sim$10 km based on a nearly horizontal band of microearthquakes beneath the CR (Carena *et al.* 2002). Results from GPS inversion suggest a slightly larger dip angle of $\sim$10° (Johnson *et al.* 2005), which better match our best-fitting tremor depth of 19 km.

We hypothesize that the NVT may occur on the subhorizontal décollement below the CR (Fig. 1b). This is supported not only by the tremor depth and location, but also by the correlation of the tremor timing and stressing from the Love wave displacements. As shown in Fig. 3, the NVT lights up as the Love wave displacement is to the southwest, and turns off as the displacement goes to the opposite direction. Since Love wave amplitude diminishes with depth, the vertical gradient in displacement would result in horizontal shear in the displacement direction (e.g. Rubinstein *et al.* 2007). Due to the unique geometry between the Kunlun earthquake and Taiwan, the surface waves of the Kunlun earthquake propagate nearly perpendicular to the strike of the mountain belt. Hence, a southwest displacement in the Love wave would result in southwest movement of the upper CR relative to the underlying Eurasian plate and the Luzon Arc. This is compatible with the left-lateral plate motion from GPS data (Yu *et al.* 1997). Hence, when the Love wave displacement is to the southwest, the basal detachment fault slips and generates tremor signals. When the Love wave displacement is to the northeast, the opposite of the plate motion, NVT is inhibited.

6 DISCUSSION

Our observation of NVT triggered by the Love wave is compatible with the recent observations in Vancouver Island (Rubinstein *et al.* 2007) and California (Gomberg *et al.* 2008; Peng *et al.* 2008). These results suggest that a simple frictional failure criterion is sufficient to explain the triggered tremor phenomenon, and support the conclusions that NVT is generated by shear slip on the plate interface (Shelly *et al.* 2006, 2007). Because the lithostatic stresses at the depth where tremor occurs are $\sim$10^4 times larger than the dynamic stress ($\sim$60 KPa) associated with the teleseismic waves, we infer that the basal detachment fault is very weak. This is consistent with a recent estimate of the effective coefficients of friction (0.04–0.1) for the basal detachment fault in Taiwan (Suppe 2007), which are an order of magnitude less than most laboratory friction coefficients (0.6–0.85).

Although NVT and slow-slip events have been observed along the circum-Pacific subduction zones (e.g. Obara 2002; Schwartz

& Rokosky 2007) and the SAF system in California (Nadeau & Dolenc 2005; Gomberg *et al.* 2008; Peng *et al.* 2008), this is the first time that (triggered) NVT is observed along a continental-arc-type collision environment. We hypothesize that the Love waves of the Kunlun earthquake trigger slow-slip events on the basal detachment, partially generating tremor signals observed at many stations. Since there are dense GPS and other geodetic instruments covering the Island of Taiwan, it is worth examining the relevant data for possible geodetic evidence of triggered slip during the surface waves of the Kunlun earthquake. In addition, it would be interesting to search for regular tremor and slow-slip events in Taiwan from the continuous seismic and geodetic recordings.

Many studies have suggested that fluids from the dehydration processes in the subducted slabs are responsible for the generation of tremor and slow-slip events (Obara 2002; Kao *et al.* 2005). Near-lithostatic fluid pressures have also been proposed to explain the existence of large overthrust faulting (Hubbert & Rubey 1959). However, the measured pore-fluid to lithostatic pressure ratio is typically in the range of 0.4–0.7, at least in the front 30 km of the wedge in western Taiwan (Davis *et al.* 1983; Suppe 2007). This indicates that high fluid pressure may help but is not sufficient alone to cause the weak fault strength and generate tremor beneath the CR in Taiwan. Further studies are needed to quantify the role of fluids in controlling the weakness and frictional behaviour of the detachment fault (e.g. Suppe and Yue 2008).

The frictional behaviours of large crustal faults and subduction zones (Scholz 1998) evolve with depth. The upper transition from stable (creep) to unstable frictional behaviour has been associated with a change from velocity strengthening to velocity weakening (Marone & Scholz 1988). The lower transition occurs on the downward extension of the seismogenic zone at the depth corresponding to the onset of the plasticity of the most ductile material. A typical temperature for the onset of the crystal plasticity of quartz (i.e. the most ductile of the major minerals in granite) is about 350°C (Scholz 1998). If we assume that this is the temperature at the depth where tremor was triggered, the corresponding geothermal gradient is about 18°C km^{-1}, which is somewhat lower than the range of 30–90°C km^{-1} around the CR estimated by Chi & Reed (2008). This could be caused by different rock types (and hence different transition temperature) on the detachment fault. Alternatively, it may suggest that temperature (and depth) may not be the primary control on the tremor and slow-slip processes (e.g. McCaffrey *et al.* 2008).

In studies where tremor depth is relatively well constrained (e.g. Shelly *et al.* 2006; Miyazawa & Brodsky 2008), regular and triggered NVT appears to occur near the lower transition zone. Our observation of triggered tremor suggests that such transition may exist on the basal detachment fault as well (Fig. 1b). Since such transition is a universal feature for many crustal faults and subduction zones (Scholz 1998), we hypothesize that NVT may exist at a wide range of active tectonic environments.

We note that NVT is not triggered everywhere by large teleseismic events, indicating that specific conditions (e.g. temperature, pressure, rock type and frictional properties) are needed for their occurrence. However, the relatively low triggering threshold, together with the simple fault geometry (e.g. Fig. 1b), suggests that the triggered tremor phenomenon is more widespread than previously thought. Observing triggered tremor at diverse tectonic environments will help us to better quantify the triggering mechanisms and necessary conditions, improve our understanding of fundamental processes at the deep root of active faults, and provide a better understanding of seismic hazard associated with these events.

REFERENCES

Carena, S., Suppe, J. & Kao, H., 2002. Active detachment of Taiwan illuminated by small earthquakes and its control of first-order topography, *Geology,* **30,** 935–938.

Chen, C.-H., Wang, W.-H. & Teng, T.-L., 2001. 3D velocity structure around the source area of the 1999 Chi-Chi, Taiwan, earthquake: before and after the mainshock, *Bull. seism. Soc. Am.,* **91,** 1013–1027.

Chi, W.C. & Reed, D.L., 2008. Evolution of shallow crustal thermal structure from subduction to collision: an example from Taiwan, *Geol. Soc. Am. Bull.,* **120,** 679–690, doi:10.1130/B26210.1.

Davis, D., Suppe, J. & Dahlen, F.A., 1983. Mechanics of fold-and-thrust belts and accretionary wedges, *J. geophys. Res.,* **88,** 1153–1172.

Dominguez, S., Avouac, J.-P. & Michel, R., 2003. Horizontal coseismic deformation of the 1999 Chi-Chi earthquake measured from SPOT satellite images: implications for the seismic cycle along the western foothills of central Taiwan, *J. geophys. Res.,* **108,** 2083, doi:10.1029/2001JB000951.

Gomberg, J., Rubinstein, J.L., Peng, Z., Creager, K.C., Vidale, J.E. & Bodin, P., 2008. Widespread triggering of non-volcanic tremor in California, *Science,* **319,** 173.

Hill, D.P. & Prejean, S.G., 2007. Dynamic triggering, in *Treatise on Geophysics,* pp. 257–292, ed. Schubert, G., Vol. 4: Earthquake Seismology, ed. Kanamori, H., Elsevier, Amsterdam.

Hubbert, M.K. & Rubey, W.W., 1959. Mechanics of fluid-filled porous solids and its application to overthrust faulting I, *Geol. Soc. Am. Bull.,* **70,** 115–166.

Jaeger, J.C. & Cook, N.G.W., 1979. *Fundamentals of Rock Mechanics,* 3rd edn, Chapman and Hall, New York.

Johnson, K.M., Segall, P. & Yu, S.B., 2005. A viscoelastic earthquake cycle model for Taiwan, *J. geophys. Res.,* **110,** doi:10.1029/2004JB003516.

Kao, H., Shan, S., Dragert, H., Rogers, G., Cassidy, J.F. & Ramachandran, K., 2005. A wide depth distribution of seismic tremors along the northern Cascadia margin, *Nature,* **436,** 841–844.

Lin, A., Fu, B., Guo, J., Zeng, Q., Dang, G., He, W. & Zhao, Y., 2002. Co-seismic strike-slip and rupture length produced by the 2001 Central Kunlun earthquake, *Science,* **296,** 2015–2017.

McCaffrey, R., Wallace, L.M. & Beavan, J., 2008. Slow slip and frictional transition at low temperature at the Hikurangi subduction zone, *Nature Geosci.,* **1,** 316–320, doi:10.1038/ngeo178.

Marone, C. & Scholz, C.H., 1988. The depth of seismic faulting and the upper transition from stable to unstable slip regimes, *Geophys. Res. Lett.,* **15,** 621–624.

Miyazawa, M. & Brodsky, E.E., 2008. Deep low-frequency tremor that correlates with the passing surface waves, *J. geophys. Res.,* **113,** doi:10.1029/2006JB004890.

Miyazawa, M. & Mori, J., 2005. Detection of triggered deep low-frequency events from the 2003 Tokachi-oki earthquake, *Geophys. Res. Lett.,* **32,** L10307, doi:10.1029/2005GL022539.

Miyazawa, M. & Mori, J., 2006. Evidence suggesting fluid flow beneath Japan due to periodic seismic triggering from the 2004 Sumatra-Andaman earthquake, *Geophys. Res. Lett.,* **33,** L05303, doi:10.1029/2005GL025087.

Nadeau, R.M. & Dolenc, D., 2005. Nonvolcanic tremors deep beneath the San Andreas Fault, *Science,* **307,** 389.

Obara, K., 2002. Nonvolcanic deep tremor associated with subduction in southwest Japan, *Science,* **296,** 1679–1681.

Peng, Z., Vidale, J.E., Creager, K.C., Rubinstein, J.L., Gomberg, J. & Bodin, P., 2008. Strong tremor near Parkfield, CA excited by the 2002 Denali earthquake, *Geophys. Res. Lett.,* submitted.

Rogers, G. & Dragert, H., 2003. Episodic tremor and slip on the Cascadia subduction zone: the chatter of silent slip, *Science,* **300,** 1942–1943.

Rubinstein, J.L., Vidale, J.E., Gomberg, J., Bodin, P., Creager, K.C. & Malone, S., 2007. Non-volcanic tremor driven by large transient shear stresses, *Nature,* **448,** 579–582.

Scholz, C.H., 1998. Earthquakes and friction laws, *Nature,* **391,** 37–42.

Schwartz, S.Y. & Rokosky, J.M., 2007. Slow slip events and seismic tremor at circum-Pacific subduction zones, *Rev. Geophys.,* **45,** doi:10.1029/2006RG000208.

Shelly, D.R., Beroza, G.C., Ide, S. & Nakamula, S., 2006. Low-frequency earthquakes in Shikoku, Japan, and their relationship to episodic tremor and slip, *Nature,* **442,** 188–191.

Shelly, D.R., Beroza, G.C. & Ide, S., 2007. Non-volcanic tremor and low-frequency earthquake swarms, *Nature,* **446,** 305–307.

Suppe, J., 2007. Absolute fault and crustal strength from wedge tapers, *Geology,* **35**(12), 1127–1130; doi:10.1130/G24053A.1.

Suppe, J. & Yue, L.-F., 2008. Pore-fluid pressures and crustal strength, *EGU Geophys. Res. Abstr.,* **10,** EGU2008-A-01970.

Yu, S.B., Chen, H.Y. & Kuo, L.C., 1997. Velocity field of GPS stations in the Taiwan area, *Tectonophysics,* **274,** 41–59.

SUPPORTING INFORMATION

Additional Supporting Information may be found in the online version of this article.

Figure S1. A record section of envelope functions for the nearest 15 stations showing the moveout of the tremor signals. The envelope function is generated by taking envelopes of 2–8 Hz bandpass-filtered seismograms, resampling at 10 samples per second, smoothing by a half width of 50 samples, and stacking three-components at each station. The dashed lines mark the *S*-wave traveltime based on a 1-D velocity model (Chen *et al.* 2001) and the best-fitting tremor location.

Figure S2. A record section of the 2–8 Hz bandpass-filtered vertical seismograms recorded by 22 stations with high signal-to-noise ratios. The seismograms are plotted against the hypocentral distances from the best-fitting tremor locations. The station names are marked on the right side. The seismograms within 80 km show clear move-out with distance. Additional tremor may occur in the northeastern Taiwan near NACB.

Figure S3. A comparison of the background seismicity (dots) and the tremor location (red star) along the cross-section AA' in Fig. 1. The seismicity is selected from the CWB catalogue with quality A or B and within 10 km along the cross-section AA'. The red arrow marks the Longitudinal Valley Fault (LVF) outlined by the dipping seismicity.

Figure S4. Moveout of the Love wave displacement recorded by the BATS stations with distance from the epicentre of the Kunlun earthquake. The blue bars mark the observed peak at each station, and the red dashed lines denote the best-fitting phase velocity of 4.1 km s^{-1}.

Please note: Wiley-Blackwell is not responsible for the content or functionality of any Supporting Information supplied by the authors. Any queries (other than missing material) should be directed to the corresponding author for the article.
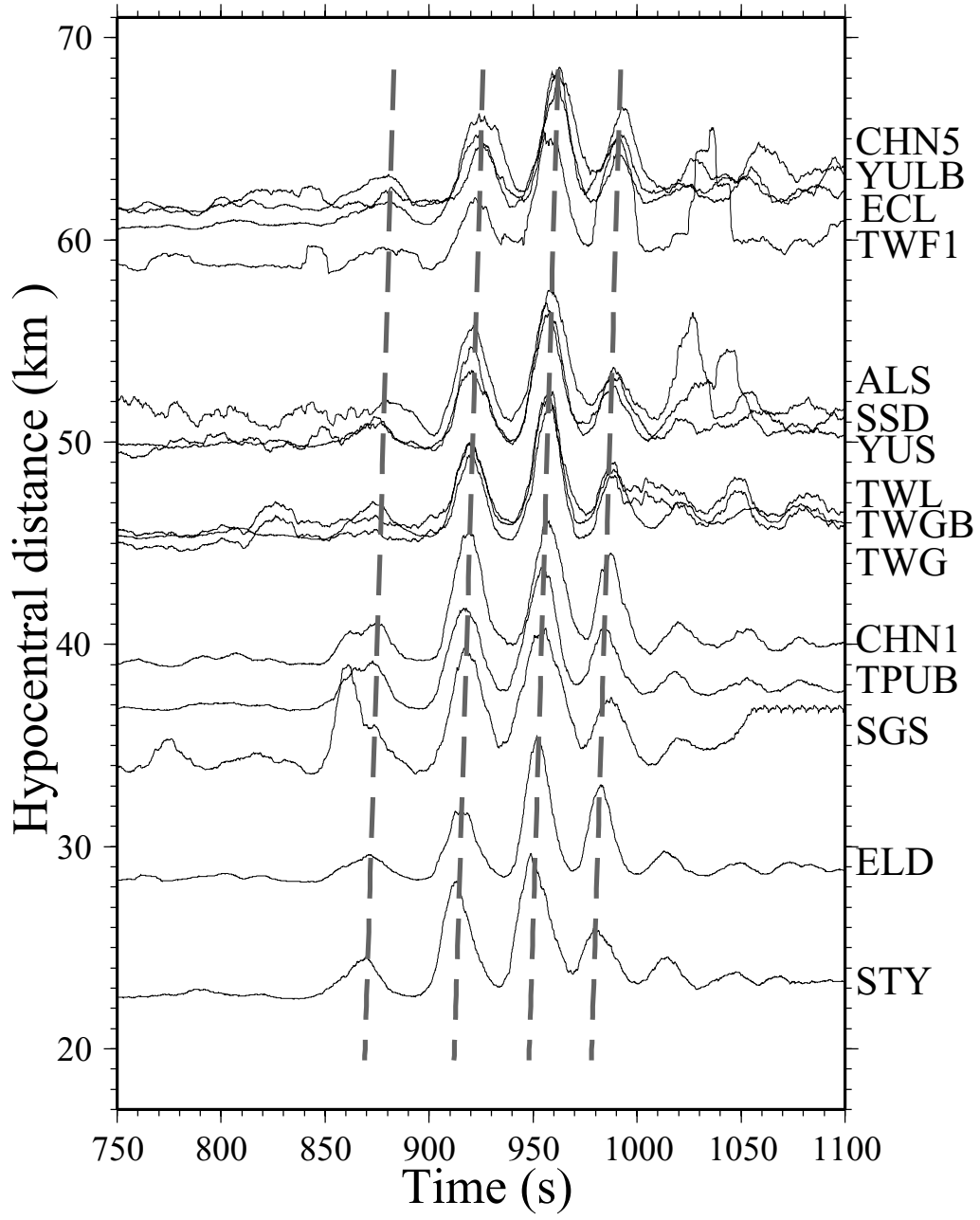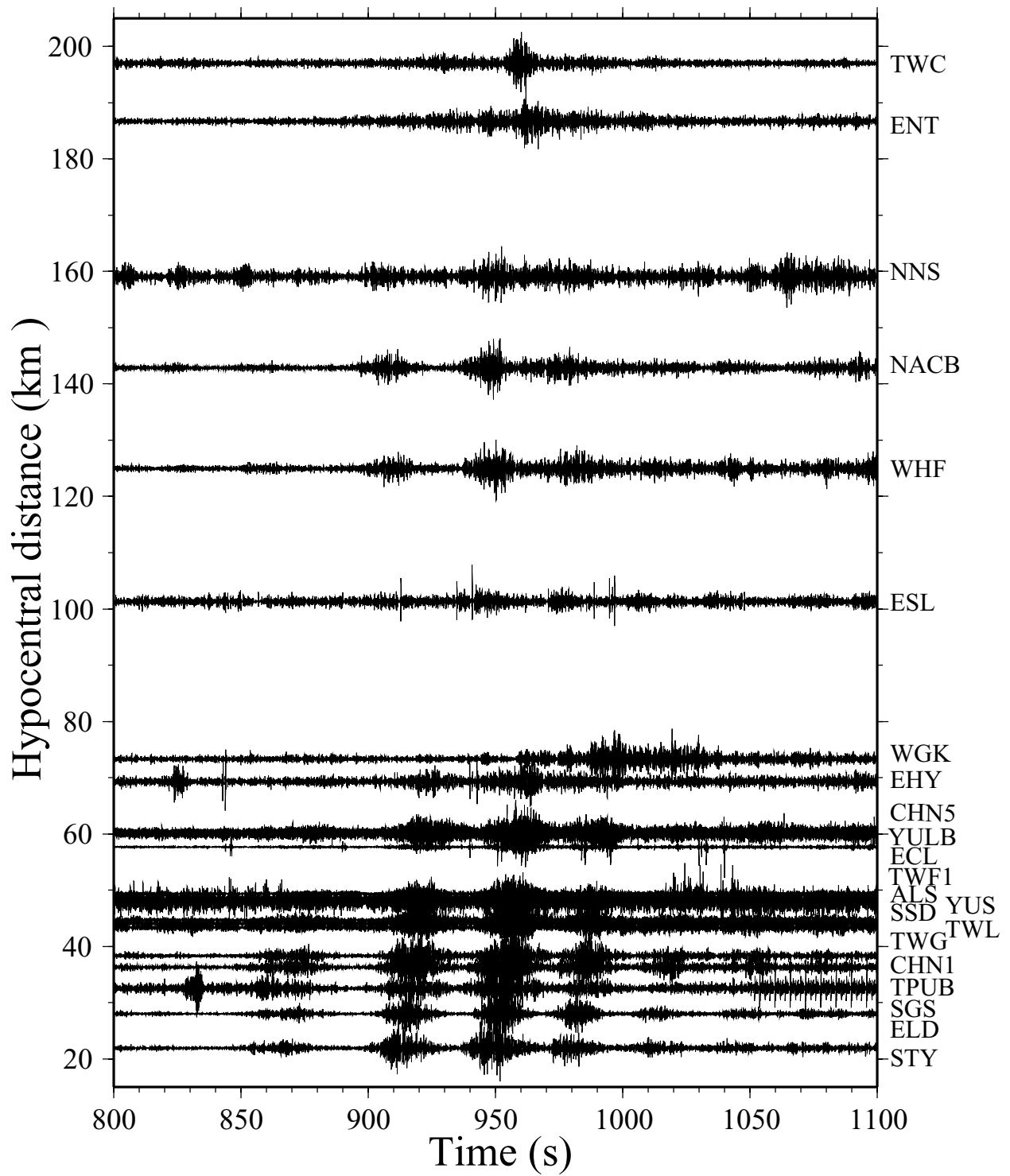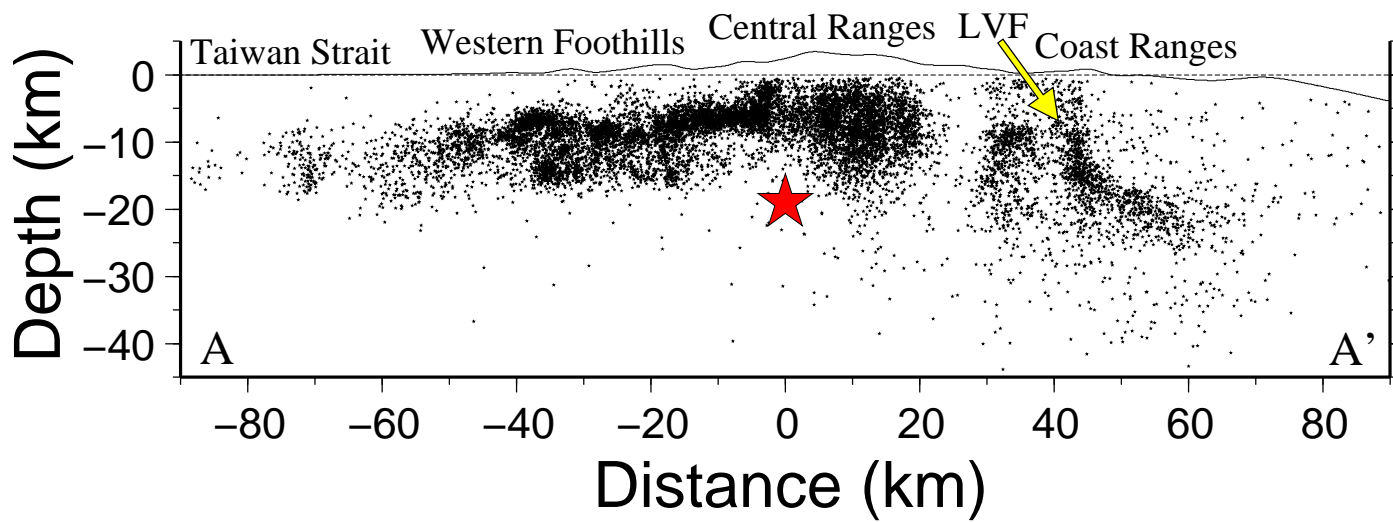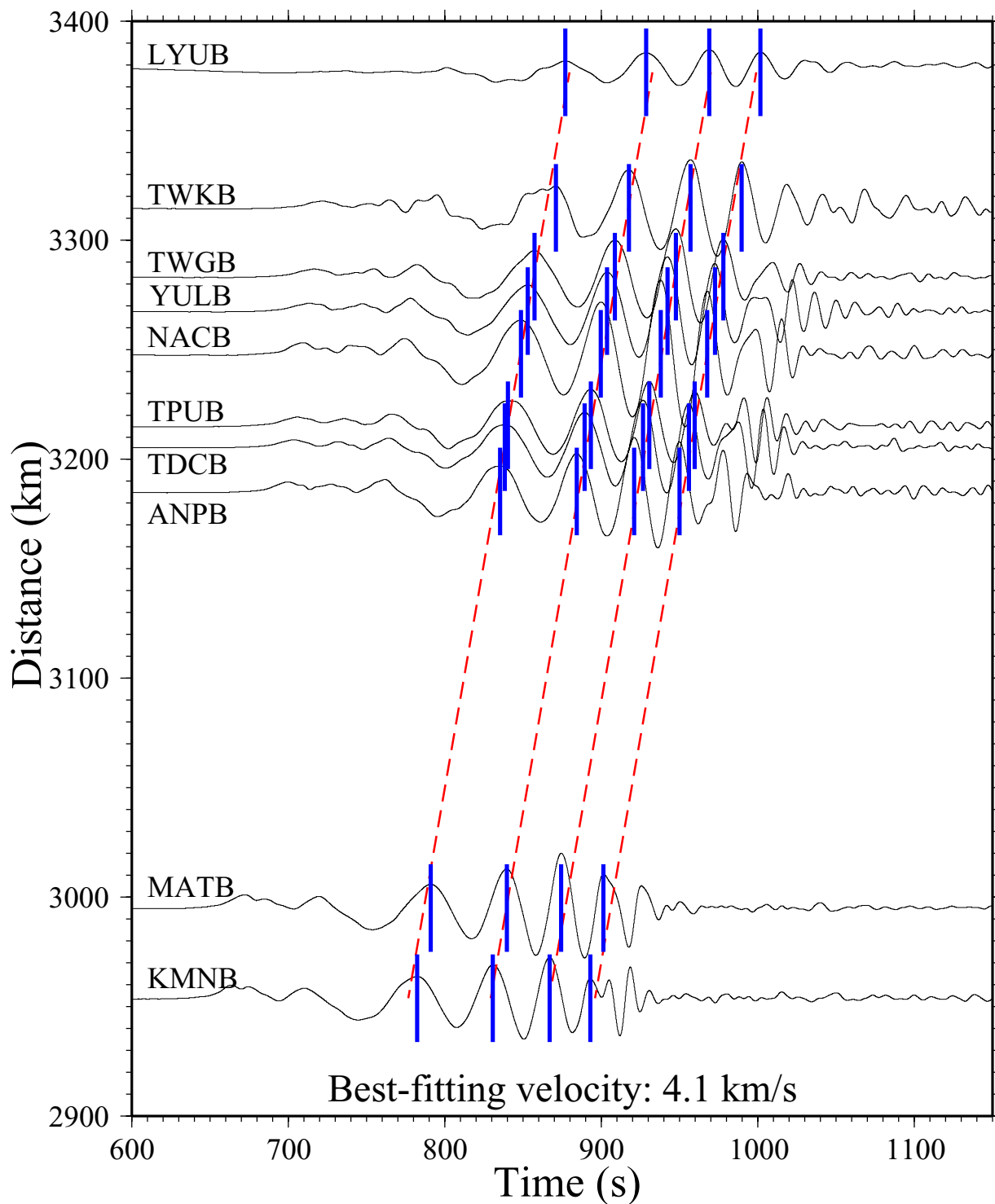
Fig. S1

Fig. S2

Fig. S3

Fig. S4